Journal of Pharmaceutical Investigation
https://doi.org/10.1007/s40005-024-00682-x

ORIGINAL ARTICLE

Formulation and evaluation of ivermectin-loaded dissolving microarray patches for rosacea disease

Qonita Kurnia Anjani[1,2] · Sara Demartis[3] · Natalia Moreno-Castellanos[4] · Elisabetta Gavini[5] · Ryan F. Donnelly[1]

Received: 7 February 2024 / Accepted: 13 May 2024

Abstract

Purpose This investigation aims to develop and characterise dissolving microarray patches (MAPs) loaded with ivermectin (IVM) for rosacea therapy.

Methods Tween® 80 and Soluplus® were evaluated to enhance the water solubility of IVM powder. Three dissolving MAPs were fabricated using a two-layer casting method, pure IVM-loaded (F1), IVM-Tween® 80 (F2), and IVM-Soluplus® (F3) loaded patches. Formulations were evaluated for drug content, in vitro and ex vivo mechanical performances, ex vivo skin dissolution time, dermatokinetics, in vitro biocompatibility and activity against rosacea.

Results IVM solubility in water was improved with surfactants, reaching 1206.42 ± 53.78 and 130.78 ± 12.78 µg/mL in Tween® 80 and Soluplus® solutions, respectively. The MAPs, featuring bubble-free, perfectly shaped pyramidal needles of approximately 800 µm, exhibited considerably higher IVM content in F2 and F3 than in F1 (2.31 ± 0.26 mg for F1, 3.58 ± 0.15 mg for F2, and 3.19 ± 0.22 mg for F3). All formulations demonstrated mechanical robustness and penetrated the skin to a depth of 650 µm. The highest IVM deposition in the skin at 24 h was achieved by F2, selected as the lead formulation (F1 = 1456.35 ± 266.90 µg; F2 = 2165.24 ± 130.13 µg; F3 = 1684.74 ± 212.09 µg). Furthermore, F2 and F3 provided faster IVM deposition, most likely due to the quicker dissolution rate of microneedles in the skin. F2 proved biocompatible to skin cells in vitro and effectively inhibited the inflammatory cascade associated with rosacea diseases.

Conclusion This study encourages further investigation into IVM-loaded dissolving MAPs formulated with Tween® 80 for rosacea therapy.

Keywords Ivermectin · Rosacea · Dissolving microarray patches · Tween® 80 · Soluplus®

Introduction

Ivermectin (IVM) belongs to the poorly soluble drug category, derived from the antiparasitic class of macrocyclic lactones called avermectins. As an endectocide, IVM actively combats various parasitic infections and plays a crucial role in global disease-elimination programs (Ōmura and Crump 2004; Ashour 2019). The scope of IVM's activities is expanding, with preliminary studies indicating its potential antiviral, antimalarial, antimetabolic, and anticancer effects (Martin et al. 2021; Mathachan et al. 2021). In recent decades, IVM has become notable for its effectiveness in treating dermatological diseases, including scabies, pediculosis, demodicosis, and, notably, rosacea. The Food and Drug Administration approved a topical IVM 1% w/w cream in 2014 for the once-daily treatment of rosacea. This approval was based on the cream's ability to reduce inflammation associated with rosacea, leading to an improvement

✉ Ryan F. Donnelly
r.donnelly@qub.ac.uk

1 School of Pharmacy, Medical Biology Centre, Queen's University Belfast, 97 Lisburn Road, Belfast BT9 7BL, UK

2 Faculty of Pharmacy, Universitas Megarezky, Jl. Antang Raya No. 43, Makassar 90234, Indonesia

3 Department of Chemical, Physical, Mathematical and Natural Sciences, University of Sassari, Piazza Università 21, Sassari 07100, Italy

4 Basic Science Department, Faculty of Health, Universidad Industrial de Santander, Bucaramanga 680001, Colombia

5 Department of Medicine, Surgery and Pharmacy, University of Sassari, Piazza Università 21, Sassari 07100, Italy

Published online: 03 June 2024

in patient quality of life (Zargari et al. 2016; Mathachan et al. 2021). Rosacea, a chronic inflammatory skin disorder affecting approximately 5.5% of adults globally (van Zuuren et al. 2021), primarily impacts the central region of the face. It manifests as recurrent episodes of flushing, persistent erythema, inflammatory lesions, telangiectasia and changes in skin surface over time (Kim 2020).

While the exact pathogenesis of rosacea is not fully clear, it is believed to result from a complex interplay of various pathways involving dysregulation of immune and neurocutaneous mechanisms, genetics, microorganisms, and environmental factors. Immune activation triggered by microbes increases cytokine production and antimicrobial peptides, leading to pustules, papules, pain, and increased vascular responsivity. Individuals with rosacea often experience emotional distress, impacting their quality of life, social interactions, and psychological well-being (Ahn and Huang 2018; van Zuuren et al. 2021). IVM's role in treating rosacea stems from its dual antiparasitic activity against the *Demodex* mite, a commensal of facial skin, the density of which is higher in rosacea patients (Ní Raghallaigh et al. 2012). Additionally, IVM exhibits anti-inflammatory activity by upregulating anti-inflammatory cytokines and inhibiting proinflammatory ones. When applied as a topical 1% cream once daily, IVM has been shown to significantly decrease the mite population and gene expression for proinflammatory substances after 6 weeks of treatment (Schaller et al. 2017). Unlike orally administered IVM, which is associated with neurological disorders, topical IVM has generally shown no severe side effects. A 0.5% w/w IVM lotion was found to be less irritating than normal saline and sodium dodecyl sulphate solutions, with minimal evidence of skin irritation or sensitisation (Zargari et al. 2016; Karthikeyan et al. 2022).

Despite the curative benefits, IVM cream faces limitations, due to its pharmaceutical dosage form. Supplied in tubes, each gram contains 10 mg of IVM, and the prescribed pea-size amount for rosacea lesions implies wide variability in medication application (Raedler 2015). The absence of a single-unit dosage poses risks of poor therapeutic adherence, leading to inferior health outcomes and increased costs for patients (Menditto et al. 2020). Accurate dosing, particularly for antimicrobials, is crucial to mitigate resistance risks (Ashour 2019; Wicha et al. 2021). Another drawback is the variable therapy duration of 21 to 112 days, further challenging therapeutic adherence (Deeks 2015; Schaller et al. 2017; Menditto et al. 2020). Topical vehicles, in general, are poorly accepted by patients (Menditto et al. 2020; Barnes et al. 2021), being influenced by organoleptic properties and ease of use. From this perspective, dermatological research must focus on reformulating existing medications to enhance administration, bioavailability, ease of use, and treatment outcomes (Menditto et al. 2020; Barnes et al. 2021). Rosacea treatment has benefited from developing novel delivery systems for well-known active compounds (van Zuuren et al. 2021; Paiva-Santos et al. 2023).

Dissolving microneedle array patches (DMAPs) represent a well-studied platform for cutaneous and percutaneous drug delivery. These patches consist of numerous water-soluble and biodegradable polymeric microneedles (MNs) that penetrate the *stratum corneum* barrier and release the drug directly into the skin upon MN dissolution. Notably, MNs are typically shorter than 1 mm, minimizing stimulation of nociceptors or blood vessels (Zhang et al. 2021; Vitore et al. 2023; Vora et al. 2023). DMAPs offer several advantages in treating various skin diseases compared to cream formulations (Yang et al. 2021; Chen et al. 2022; Qu et al. 2022). Unlike creams, DMAPs enhance drug deposition at the pathological site through reversible microchannels created upon skin insertion. For conditions like Rosacea, which requires delivery of the drug to the epidermis, dermis, and subcutaneous layers due to the presence of Demodex mites in hair follicles (MacLeod et al. 2009), MAPs can penetrate and reach these layers more effectively than topical creams (Martel et al. 2024), facilitating release of the drug to overcome Demodex infections. IVM, with its high molecular weight and poor water solubility, may necessitate prolonged therapy duration. Additionally, DMAPs allow for tailored drug dosage and delivery rates by modifying MN design, material, and drug-containing formulation, facilitating controlled and sustained release with reduced administration frequency (Jung and Jin 2021; Gowda et al. 2023). These features make DMAPs an easy-to-use, painless, and non-invasive device with increased acceptability (Li et al. 2021; Sartawi et al. 2022). The present study focuses on developing DMAPs loaded with IVM to offer a more acceptable and efficacious dosage form for managing rosacea compared to currently available creams. Initially, the study aimed to enhance IVM solubility by testing two surfactants, Tween®80 and Soluplus®. Subsequently, DMAPs were fabricated, and their mechanical properties, as well as in vitro and ex vivo performances, were evaluated. The delivery efficiency of IVM-loaded DMAPs was assessed through an ex vivo dermatokinetic study to evaluate the amount of IVM deposited in each layer of skin at predetermined times, while the biocompatibility and efficacy of selected DMAPs against rosacea biomarkers were tested in vitro.

Materials and methods

Materials

Ivermectin (IVM) (purity, 95%) and Tween® 80 were purchased from Tokyo Chemical (Oxford, UK). Soluplus® was generously provided by BASF (Ludwigshafen, Germany). Polyvinylpyrrolidone (PVP) 90 kDa (Plasdone™ K-29/32) was obtained from Ashland (Kidderminster, UK). Dulbecco's Modified Eagle's medium (DMEM), fetal bovine serum (FBS), and the 3-(4,5-dimethylthiazol-2-yl)-2,5-diphenyltetrazolium bromide (MTT) assay kit, along with dimethyl sulfoxide (DMSO), were sourced from Sigma Aldrich (St. Louis, MO, USA). The human epidermal keratinocytes (HaCaT) cell line was acquired from ATCC. The enzyme-linked immunosorbent assay (ELISA) analysis kit was procured from R&D Systems (Minneapolis, MN, USA). All other reagents, which were of analytical grade, were purchased from Sigma-Aldrich (Dorset, UK) or Fisher Scientific (Loughborough, UK). The full-thickness neonatal porcine skin used in the study was sourced from stillborn piglets within 24 h *post-mortem* and stored frozen at -20 °C before experimentation.

High-performance liquid chromatography (HPLC) analysis

IVM sample analysis was performed using a reversed-phase high-performance liquid chromatography (HPLC) system. The specific instrument was the Agilent Technologies 1220 Infinity compact LC series system (Agilent Technologies UK Ltd, Stockport, UK), which is equipped with a UV detector. For chromatographic separation, an XSelect CSH C18 column was employed. The column had a 3.0 mm internal diameter, 150 mm length, 3.5 µm particle size, and a pore size of 130 Å. Before the main column, a VanGuard® cartridge with similar chemistry (3.9 mm internal diameter, 5 mm length) was used for column protection. The mobile phase consisted of a mixture of 0.1% v/v trifluoroacetic acid and acetonitrile in a ratio of 2:98. The eluent was pumped through the column at a 0.6 mL/min flow rate. The HPLC samples containing IVM were injected into the system with a volume of 20 µL. The UV detector was set to monitor the analyte at a wavelength of 248 nm. The overall sample analysis time was 12 min, during which the separation and quantification of IVM took place.

Enhancement of IVM water solubility

Saturation and solubility test of IVM in surfactant solutions

An excess amount of IVM was separately added to an Eppendorf tube containing 2 mL of aqueous surfactant solutions (Tween® 80 0.5% w/v and Soluplus® 0.5% w/v) or deionised water, followed by vortexing for 1 min at 2,500 rpm. The prepared samples were incubated in a shaker incubator (Jeio Tech ISF-7100, Medline Scientific, Chalgrove Oxon, UK) at 37 °C and 1,500 rpm for 24 h. After incubation, the samples underwent centrifugation at 14,800 rpm for 15 min to separate the non-solubilised IVM, followed by filtration using a 0.45 µm nylon membrane. The filtered samples were analysed by HPLC. If necessary, samples were diluted in PBS (pH 7.4) before analysis. Three replicate measurements were performed to obtain the results ($n = 3$).

Determination of contact angle of surfactant solutions with IVM

The contact angle between IVM and surfactant solutions (Tween® 80 0.5% w/v and Soluplus® 0.5% w/v) was measured using an Attension Theta optical tensiometer (Biolin Scientific, Gothenburg, Sweden), following methodologies outlined in previously published studies (Anjani et al. 2022d). A 50 mg amount of IVM was accurately weighed and compressed into a tablet using 4 tonnes for 1 min to ensure a level surface. The sessile drop method was then employed to determine the contact angle between the IVM tablet and surfactant solutions (Tween® 80 and Soluplus®) at a concentration of 0.5% w/v. At the same time, deionised water was used as the control. A 4 µL droplet of each surfactant solution (0.5% w/v) or water was carefully placed onto the surface of the IVM tablet, and the wetting angle was precisely measured 30 s after the droplet deposition. Subsequently, the collected data underwent comprehensive analysis and interpretation using OneAttension software. Three replicate measurements were performed to obtain the results ($n = 3$).

Morphology, size and polydispersity index of IVM in surfactant solutions

Ivermectin (2 mg) was separately dispersed in a glass vial containing either 4 mL of surfactant solutions (0.5% w/v Tween® 80 and 0.5% w/v Soluplus®) or deionised water. The dispersion was homogenised using a vortex at 2,500 rpm for 1 min. For morphological evaluation, approximately 100 µL of each mixture was deposited onto adhesive carbon tape and left for 24 h to allow water evaporation before visualisation using a TM3030 microscope (Hitachi, Krefeld,

Germany). To determine particle size and polydispersity index (PDI), each mixture was transferred into a disposable cell (12 mm length, 45 mm height, 12 mm width) for analysis *via* dynamic light scattering (DLS). The measurements were conducted using a NanoBrook Omni analyser (Brookhaven, NY, USA) at 25 °C, allowing for a 3-minute equilibration time. Three replicate measurements were performed to obtain the results ($n = 3$).

Fabrication of DMAPs

Three different formulations of DMAPs loaded with IVM were prepared using a double-casting method (Demartis et al. 2022). As a general procedure, the needle tips (first layer) were obtained after dispersing IVM in a polymeric solution containing 20% w/w PVA (9–10 kDa), 20% w/w PVP (58 kDa) and, eventually, surfactants (Tween® 80 or Soluplus®), as specified in Table 1. The baseplate layer of the patches (second layer) consisted of an aqueous polymeric solution of 30% w/w PVP (90 kDa) and 1.5% w/w glycerol. To form the first layer, 50 mg of each drug-containing mixture was poured into a poly(dimethylsiloxane) mould with dimensions of 16 × 16 pyramidal-cuboidal needles. The needles had a density of 850 µm height, 300 µm width at the base, 300 µm interspacing, and a patch area of 0.36 cm^2. The moulds were placed in a positive pressure chamber at 4 bar for 5 min. Excess formulation from the first layer was carefully removed using a spatula, and the moulds were placed for 30 min inside the positive pressure chamber at 4 bars. Next, elastomer rings with an external diameter of 23 mm, internal diameter of 18 mm, and a thickness of 3 mm were attached on top of the moulds using a glue solution prepared from an aqueous blend of 40% w/w PVA (9–10 kDa). The moulds were allowed to dry at room temperature for 6 h. Subsequently, 850 µL of the second layer, consisting of an aqueous blend of 30% w/w PVP (90 kDa) and 1.5% w/w glycerol, was poured into the moulds. The moulds were then centrifuged at 3,500 rpm for 10 min. After centrifugation, the moulds were dried at room temperature for 24 h. The sidewalls formed during the drying process were removed using scissors, and the moulds were further dried at 37 °C for 12 h.

Table 1 Formulation for dissolving MAP preparation

Components (mg in 100 mg of aqueous mixture)	F1	F2	F3
Ivermectin	30 mg	30 mg	30 mg
Aqueous polymer blend (PVA (9–10 kDa and PVP (58 kDa)) (20% w/w)	30 mg	30 mg	30 mg
Deionised water	40 mg	-	-
Tween® 80 solution (0.5%w/v)	-	40 mg (containing 0.2 mg)	-
Soluplus® solution (0.5%w/v)	-	-	40 mg (containing 0.2 mg)

Characterisation of DMAPs

Drug content

The drug content within DMAPs was evaluated by first dissolving the formulation in 4 mL of deionised water. The dissolution process was promoted by subjecting the DMAP to a sonication cycle of 30 min using a bath sonicator. Then, 4 mL methanol was added to solubilise IVM, and the sample was further sonicated for 30 min. The final mixture was subjected to a centrifugation cycle of 14,500 rpm for 15 min; afterwards, the supernatant was sampled and analysed *via* HPLC. Three replicate measurements were performed to obtain the results ($n = 3$).

Mechanical resistance

The architecture and appearance of the DMAPs were observed using an optical microscope (Leica EZ4 D, Leica Microsystems, Milton Keynes, UK) and scanning electron microscope (SEM) (Tabletop Microscope TM3030, Hitachi, Krefeld, Germany). The resistance of the needles under compression was ascertained using a TA-TX2 Texture Analyser (TA) (Stable Microsystems, Haslemere, UK) using previously-reported parameters (Anjani et al. 2023b). Upon exposure to a compressive force of 32 N, changes in needle height were estimated using Eq. (1).

$$MAPs\ height reduction\ (\%) = \frac{H_{initial} - H_{after}}{H_{initial}} \times 100\% \quad (1)$$

$H_{initial}$ is the original needle height, and H_{after} is the post-compression. Three replicate measurements were performed to obtain the results ($n = 3$).

Insertion capability

The insertion profiles of the DMAPs into Parafilm® M and ex vivo neonatal porcine skin were investigated using an EX-101 optical coherence tomography (OCT) microscope (Michelson Diagnostics Ltd., Kent, UK), as reported previously (Anjani et al. 2021). Before the experiment, the skin was pre-equilibrated in phosphate buffer saline (PBS) (pH 7.4) for 30 min. Upon acquiring the OCT images, the insertion depth of the needles was visualised and calculated using ImageJ® software (National Institutes of Health, Bethesda,

MD, USA). Three replicate measurements were performed to obtain the results ($n = 3$).

Ex vivo dissolution time in skin

Ex vivo dissolution in the skin was assessed (Anjani et al. 2022b). Before the experiment, the skin was pre-equilibrated in phosphate-buffered saline (PBS) (pH 7.4) for 30 min. Briefly, each DMAP formulation was inserted into the excised full-thickness neonatal porcine skin using manual thumb pressure. A 15 g cylindrical stainless-steel weight (diameter 1.4 cm, height 1.0 cm, weight 15.0 g) was placed atop the DMAPs to avoid expulsion during the study. The plate was closed and stored at 37 °C for 1 h and 3 h. After this time, the morphology of DMAPs was observed under the digital microscope following DMAP detachment from the skin.

Ex vivo dermatokinetic studies

Dermatokinetic studies using excised full-thickness neonatal porcine skin were performed to study the migration of IVM through the skin when delivered by DMAPs (Demartis et al. 2022). This work used vertical Franz diffusion cells (Permergear, Hellertown, PA, USA). Using cyanoacrylate adhesive (Stick it® super glue, PLDZ Pattison House, Dublin, Ireland), the excised skin was attached to the donor component of the apparatus. The receiver fluid used was degassed PBS at 37 °C. Using a thermostatically regulated water bath, the experimental set-up was maintained at 37 ± 1 °C. In addition, the receiver solution was stirred at a constant rate of 600 rpm. IVM-loaded DMAPs were applied to the excised skin under manual pressure for 0.5 min before being clamped to the receiver compartment. Once inserted, the DMAPs were secured using a stainless-steel cylindrical weight. As a comparison, a commercial IVM cream, efacti® cream (containing 10 mg/g IVM from Galderma, Milan, Italy) was used as a control. To reduce the risk of the receiver fluid evaporating throughout the experiment, the sampling arm and the donor component were meticulously sealed using Parafilm® M. The Franz cells were disassembled at pre-determined time points, and 200 µL of the receiver solution was sampled, filtered, and analysed *via* HPLC. Skin samples were heat treated at 60 °C for 5 min to facilitate the separation of the epidermis and dermis (Cárcamo-Martínez et al. 2021). Upon separating, the epidermal layer was homogenised in 2 mL of methanol using a Vortex® mixer (Fisons Scientific Equipment, Leicestershire, UK) for 1 min. On the other hand, the dermal tissue was homogenised in 0.5 mL of deionised water using a Tissue Lyser LT (Qiagen Ltd., Manchester, UK) (Anjani et al. 2023a). The homogenisation step was carried out at 50 Hz for 15 min. Upon homogenisation, 1 mL of methanol was added to the samples, followed by another cycle of homogenisation for 15 min. The skin samples, both epidermis and dermis layers, were subjected to a centrifugation cycle of 14,000 rpm for 15 min. Before HPLC analysis, the supernatant was collected and filtered through a 0.45 µm nylon membrane. Three replicate measurements were performed to obtain the results ($n = 3$). The percentage of delivery efficiency (DE%) was calculated after determining the amount of drug in each skin layer and the receiver compartment, using Eq. (2) below:

$$DE\% = \frac{\begin{array}{c} IVM\ in\ epidermis + IVM\ in\ dermis \\ +IVM\ in\ receiver\ compartment \end{array}}{Drug\ loading\ per\ MAP} \times 100\% \quad (2)$$

In vitro biological evaluations

Biocompatibility studies of DMAPs

The biocompatibility of IVM-loaded DMAPs and blank DMAPs was assessed using a methodology similar to a previously published approach (Anjani et al. 2022a, b; Domínguez-Robles et al. 2023). The whole DMAP samples were used without any preparation before the experiment. Human Epidermal Keratinocytes (HaCaT) cells were employed in the study, cultured in DMEM supplemented with 10% heat inactivated FBS and 1% penicillin/streptomycin. The cell cultures were maintained in a humidified 5% CO_2 incubator at 37 °C. Upon reaching confluence, the keratinocytes were seeded onto 24-well plates at a density of 5 × 104 cells per well and incubated for 72 h with the whole DMAP samples. The viability of the DMAPs was determined using the MTT assay. MTT reagent was introduced to each well, and following a 6-hour incubation, formazan crystals were dissolved using DMSO. Absorbance was measured at 540 nm using a spectrophotometer. Additionally, a LIVE/DEAD cytotoxicity assay was conducted on the keratinocytes treated with the whole DMAP samples. This involved treating the cells with a mixture of calcein-AM and ethidium homodimer-1 (EthD-1) and examining fluorescence using a fluorescence microscope at 100× magnification. Calcein-AM stains live cells green, while EthD-1 stains dead cells red. Cell proliferation was assessed by measuring the number of DNA copies in the cell cycle using the picogreen assay. DNA samples were extracted from the cells, and a DNA-binding fluorescent dye solution was employed to measure fluorescence intensity at an excitation wavelength of 480 nm and an emission wavelength of 520 nm. A standard curve using Lambda DNA was constructed to calculate the amount of

DNA. To ensure robust and reliable outcomes, six replicate measurements were conducted, contributing to the overall results ($n = 6$).

In vitro efficacy studies of DMAPs against Rosaceae biomarkers

Human Epidermal Keratinocytes were cultivated to confluence at 37 °C in a humidified atmosphere of 5% CO_2 and 95% air. Subsequently, the cells underwent treatment with cathelicidin LL-37 (3.2 µM), either alone or in combination with selected IVM-loaded DMAPs and blank DMAPs for 24 h. Following the treatment period, the supernatants were collected and subjected to ELISA using kits to quantify the production of IL1-β, IL-8, TNF-α, CXCL1, and CXCL2. The release of these cytokines and chemokines into the medium was normalised to total protein content to account for any variability in cell number. This procedure facilitated the evaluation of the impact of IVM-loaded DMAPs and blank DMAPs on the release of inflammatory mediators in human epidermal keratinocytes. Robust and reliable outcomes were ensured by conducting six replicate measurements to obtain the results ($n = 6$).

Statistical analysis

Data analysis and presentation were conducted using GraphPad Prism® version 10.1.1, developed by GraphPad Software (San Diego, California, USA). Unless explicitly stated, the results were generally presented as mean ± standard deviation (SD). An unpaired t-test was applied to determine the statistical difference between two independent groups or cohorts. This test assesses whether the observed difference between the means of the two groups is statistically significant. In cases where multiple treatment cohorts were compared for statistical significance, a one-way analysis of variance (ANOVA) was employed. ANOVA facilitates the comparison of means among three or more groups. Statistical significance was defined as a p-value less than 0.05.

Results and discussion

Enhancement of IVM water solubility

Surfactants play a crucial role in enhancing the solubility of poorly soluble drugs in an aqueous environment due to their ability to decrease the interfacial tension between a liquid and a solid (Khan et al. 2022). Non-ionic surfactants have been demonstrated to provoke fewer irritating sensations than ionic surfactants and are generally considered safer; they interact with the lipid skin by transiently increasing the fluidity of biological membranes (Hmingthansanga et al. 2022). Moreover, as reported in our previous work, the incorporation of Tween®80 in the MAP formulation was able to improve the performance as well as enhance the efficiency of delivery of both hydrophobic and hydrophilic drug models from MAP platforms (Anjani et al. 2022d). Additionally, we have previously demonstrated that the tip made by Soluplus® and drugs were biocompatible with skin cells and could help improve the skin delivery of the drugs by forming nano-sized solid dispersion (Anjani et al. 2022a, 2023d). Therefore, for this reason, Tween®80 and Soluplus® were chosen, and the solubility of IVM in the surfactant aqueous solutions (0.5% w/v), namely Tween®80 and Soluplus®, was investigated.

Tween®80, or polysorbate 80, is hydrophilic and easily soluble in water with a hydrophilic-lipophilic balance (HLB) value of 15.0 and a 428.6 g/mol molecular weight. Soluplus® is a water-soluble graft copolymer constructed from a hydrophilic moiety of polyethylene glycol residue and a lipophilic backbone of polyvinyl caprolactam/polyvinyl acetate (Attia et al. 2023); it has a HLB of 14 and a molecular weight of 118,000 g/mol. IVM solubility in water was 3.56 ± 0.019 µg/mL; in contrast, IVM solubility was 1206.42 ± 53.78 and 130.78 ± 12.78 µg/mL in Tween® 80 and Soluplus® solutions, respectively (Fig. 1a). Accordingly, the measured contact angle between water and IVM tablet was 71.5° while the contact angle for surfactant solution was 38.9° in the case of Tween® 80 and 59.8° for Soluplus® (Fig. 1d-f); this reduction was significantly different ($p < 0.05$) (Fig. 1b). Based on the sessile drop method, a contact angle lower than 90° is indicative of hydrophilic surfaces (Marmur et al. 2017); thus, the smaller contact angles indicate an increased wettability of IVM consequent to the reduced interfacial tension in the presence of surfactants, with the preeminent performance for Tween® 80 (Wang et al. 2019; Anjani et al. 2022d). Furthermore, the particle size and PDI of the dispersion of IVM in water and surfactant solutions were determined (Fig. 1c). Dispersion in water provided IVM particles higher than 1 µm (PDI 0.5 ± 0.027). In contrast, particle size significantly decreased to 17.92 ± 1.61 nm (PDI 0.214 ± 0.005) and 56.91 ± 1.34 nm (PDI 0.111 ± 0.022) ($p < 0.05$) for Tween®80 and Soluplus® dispersions, respectively, confirming the results obtained for saturation solubility and contact angles. Moreover, as shown in Fig. 1g-i, IVM was present in a crystalline form due to the incomplete dissolution of the drug in the tested media. Since this experiment was performed by dispersing 2 mg of drug in 4 mL of each media, only IVM in 0.5% w/v Tween®80 reached the concentration of saturation solubility, while IVM in water and 0.5% w/v Soluplus® did not achieve this solubility limit. Accordingly, the particle size of Tween®80 was significantly smaller ($p < 0.05$) compared

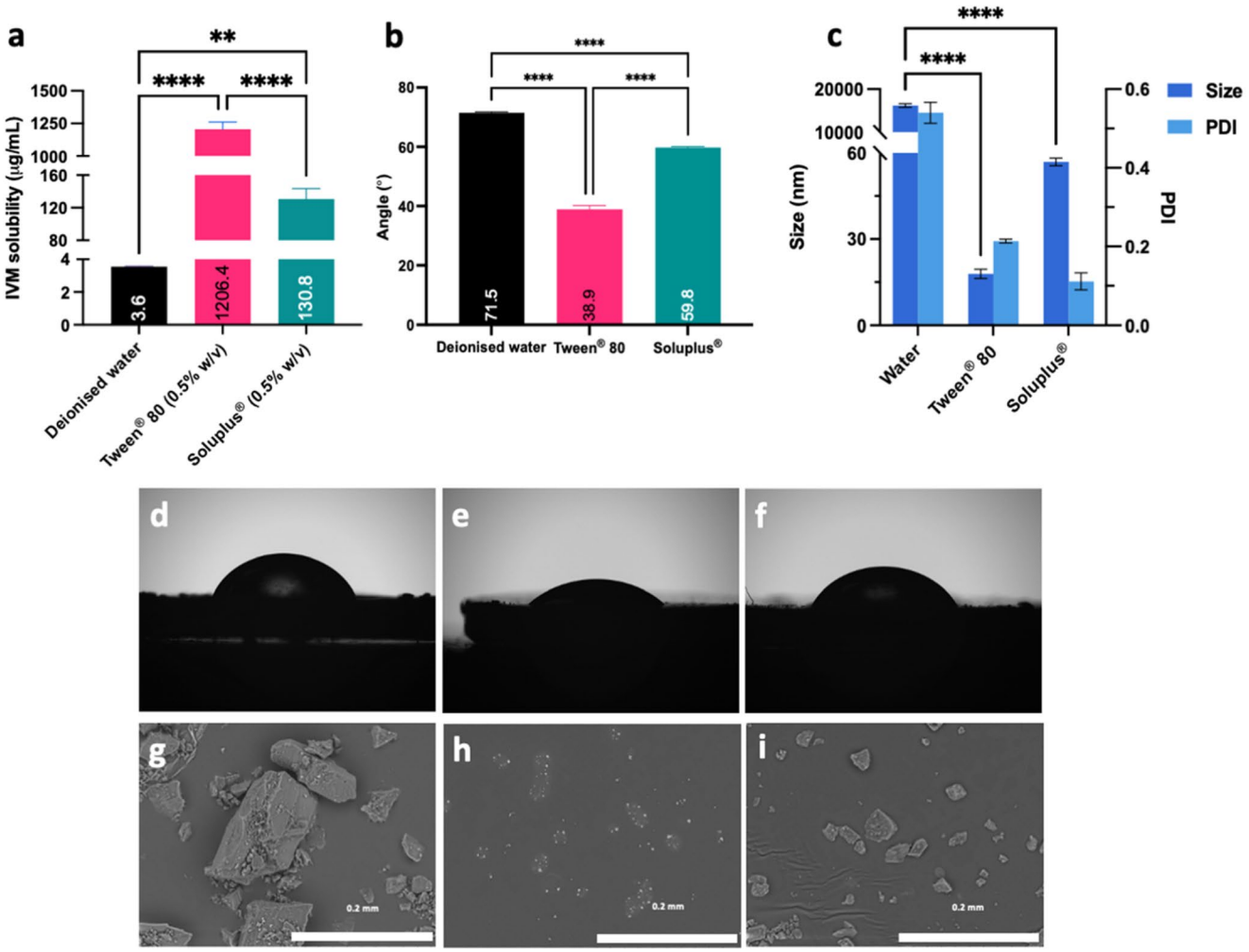

Fig. 1 Enhancement of IVM wettability. **a**: saturation solubility of IVM in water, Tween®80 (0.5% w/v) and Soluplus® (0.5% w/v) solutions (means + SD, $n = 3$). **b**: contact angle measurements between IVM tablet and water, Tween®80 (0.5% w/v) and Soluplus® (0.5% w/v) solutions (means + SD, $n = 3$). **c**: Size and PDI of IVM dispersion in water, Tween®80 and Soluplus® (means + SD, $n = 3$). **d**: contact angle between IVM and water. **e**: contact angle between IVM and Tween® 80 solution. **f**: contact angle between IVM and Soluplus® solution. **g**: SEM micrograph of IVM aqueous dispersion. **h**: SEM micrograph of IVM Tween®80 (0.5% w/v) dispersion. **i**: SEM micrograph of IVM Soluplus® (0.5% w/v) dispersion

to the other media. Despite generating smaller particle size, Tween®80 for particle size and SEM measurements did not reach complete dissolution as expected based on saturation solubility studies. This might be due to the different experimental conditions; for saturation solubility study, the samples were placed in a shaker incubator at 37 °C for 24 h, while the samples for DLS and SEM were only homogenised for 1 min. However, under these conditions, we can distinguish the different sizes of IVM particles in each media, which can explain the effect of each surfactant on IVM solubility enhancement.

Fabrication and characterisation of DMAPs

Two-layered DMAPs were fabricated using the two-step casting method illustrated in Fig. 2a. This method was chosen for DMAP manufacturing to minimise drug waste and enhance drug delivery efficiency. Indeed, this technique facilitates the accumulation of the therapeutic cargo in the tips and controls the localisation of the drug within the DMAP. A blend of PVP (MW 58 kDa) and PVA (MW 9–10 kDa) was selected as a backbone polymer for the first layer of MAP. The combination of these two polymers in a 1:1 ratio was chosen because of their low molecular weight, which allows for faster dissolution than the baseplate (made from PVP with a higher molecular weight of 90 kDa), as well as easy elimination from the body by the kidneys following needle dissolution post MAP insertion (Tekko et al. 2022). PVA and PVP interact through intermolecular hydrogen bonding between hydroxyl groups of PVA and carbonyl ones of PVP, resulting in thermodynamically miscible blends (Teodorescu et al. 2019). In the specific case of

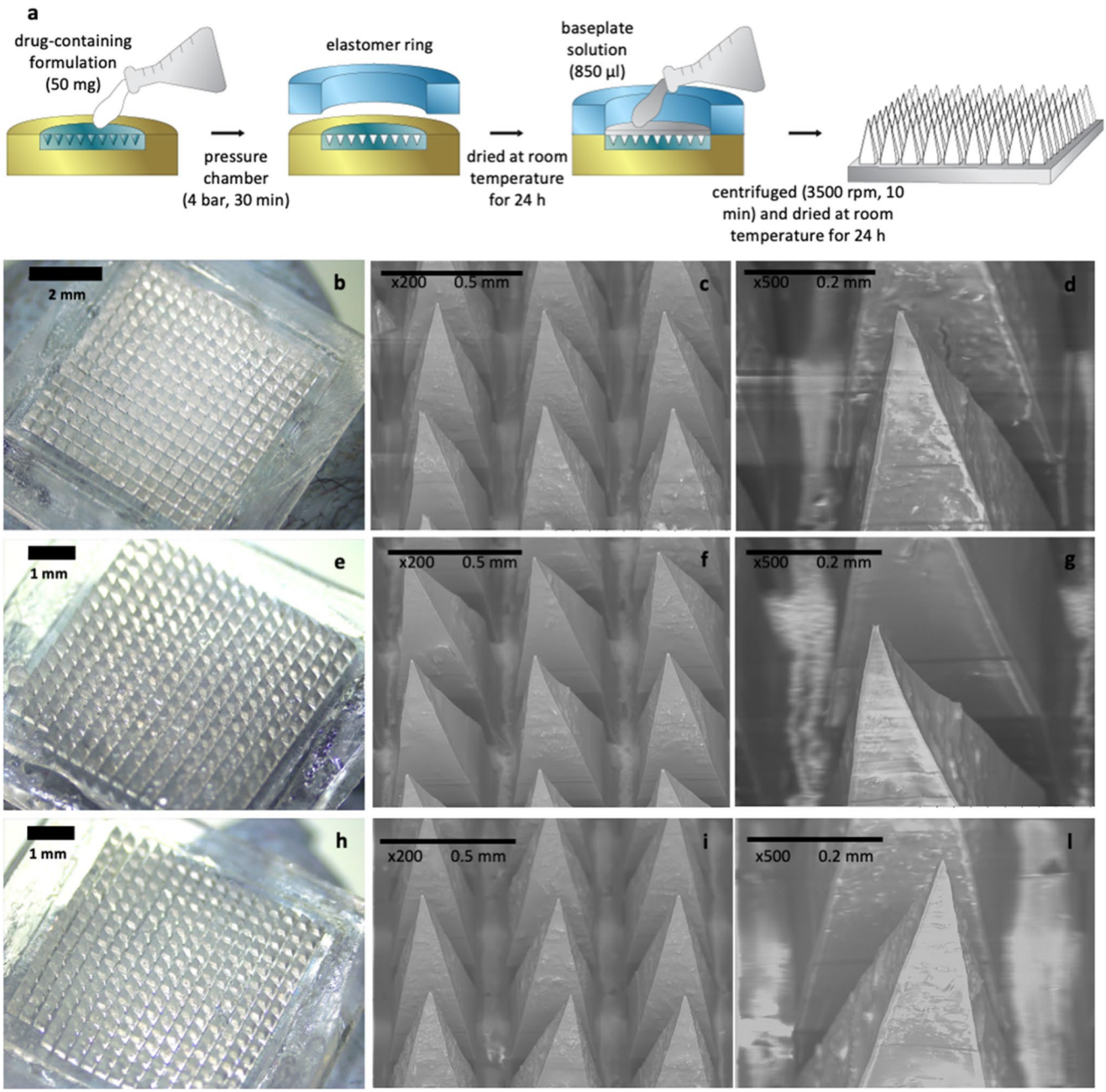

Fig. 2 Fabrication technique and microscopic evaluation of DMAPs. **a**: illustration of the two-layer casting method. **b**: top view of F1. Optical microscopy. **c-d**: SEM micrograph of F1 at different magnification (x200 and x500). **e**: top view of F2. Optical microscopy. **f-g**: SEM micrograph of F2 at different magnification (x200 and x500). **h**: top view of F3. Optical microscopy. **i-l**: SEM micrograph of F3 at different magnification (x200 and x500)

DMAPs, coupling PVA with PVP enhances the mechanical strength of the needles and assists in modulating the dissolution kinetics in the skin tissue (Wang et al. 2017). On the other hand, the higher molecular weight of PVP (MW 90 kDa) was selected as the formulation for the baseplate due to its ability to provide acceptable mechanical strength of the MAP during insertion and serve as a robust supporting base for the needles to breach the *stratum corneum* and reach the deeper layers of the skin (Tekko et al. 2022; Anjani et al. 2022c, 2023b, c, 2024).

The manufacturing technique and the use of PVA/PVP allowed us to obtain bubble-free, perfectly shaped pyramidal needles uniformly distributed on a consistent baseplate (Fig. 2b-l). Considering that IVM was suspended in the formulation used to cast the first layer, the bumps observed in the tip may be related to the undissolved drug.

The height of the microneedles was 783 ± 0.84, 800 ± 0.52, and 769 ± 0.47 µm for F1, F2, and F3 DMAPs formulations, respectively. IVM loaded in DMAPs was 2.31 ± 0.26 mg for F1, 3.58 ± 0.15 mg for F2, and 3.19 ± 0.22 mg for F3. IVM content in F2 and F3 was significantly higher than F1 (F1 vs. F2 $p < 0.001$; F1 vs. F3 $p < 0.01$), consequent to the higher saturation solubility of IVM in surfactant solutions than water.

To assess the strength of DMAPs for efficient skin penetration, mechanical properties were evaluated, specifically the height reduction when compressed against a flat surface and the insertion ability in Parafilm® M layers and skin. The percentage height reduction of DMAPs was lower than 10% for all the formulations tested, with the highest reduction in the case of F1 (F1 vs. F2 $p < 0.001$, F1 vs. F3 $p < 0.0001$) (Fig. 3a). Also, in the case of F1, the needle tips broke when submitted to the compression force (Fig. 3d), while in the case of F2 and F3, the fracture point is less evident as a propensity for bending was noted (Fig. 3e-f). This is probably due to surfactants that may soften the needle structure (Demartis et al. 2022). The observed height reduction aligns with the values reported in the literature, suggesting the fabrication of mechanically robust DMAPs (Paredes et al. 2021; Zhang et al. 2022). Accordingly, all the formulations pierced four of the eight layers of Parafilm® M during the in vitro insertion test; F2 and F3 provided the best insertion profile, completely penetrating the first two layers (Fig. 3b).

Conversely, no differences were observed for the insertion depth into ex vivo neonatal porcine skin ($p > 0.05$), as all the formulations reached approximately 650 µm depth (Fig. 3c). The thickness of the facial skin ranges between 1 and 2 mm depending on the zone ((Kim et al. 2019); however, in patients suffering from rosacea disease, the skin may be thicker than in healthy individuals due to fibrosis related to local overproduction of TGF-β1 (Cribier 2011; Vemuri et al. 2015). Furthermore, it was reported that the epidermal thickness of rosacea patients is 39.66 ± 5.04 µm (Ma et al. 2020). Considering these assumptions, the developed DMAPs appear suitable for delivering IVM in rosacea-affected skin. Figure 3g-n display the DMAPs insertion into Parafilm® M strata and skin analysed by Optical Coherence Tomography (OCT).

Ex vivo dissolution time and dermatokinetic study

The epidermis, specifically the *stratum corneum*, serves as the primary protective barrier against the permeation and retention of various compounds, including drugs. DMAPs, by piercing the *stratum corneum*, effectively overcome the skin barrier function and facilitate the deposition and permeation of the therapeutic cargo. Upon insertion into the skin, DMAPs create reversible aqueous microchannels that act as a transport pathway for the drug, which is released after microneedle dissolution (Saepang et al. 2021) (Fig. 4a). Ex vivo dissolution of DMAPs in full-thickness porcine skin increased with the insertion time (Fig. 4b-g). After 1 h, microneedles of F1 are poorly dissolved, as the pyramidal shape is easily identifiable, and after 3 h, only the base of the microneedles is visible (Fig. 4b and **e**). Conversely, F2 and F3 dissolved faster. Specifically, microneedles of F3 were almost completely dissolved after 1 h (Fig. 4c and **f**). In the case of F2, approximately half of the microneedles dissolved after 1 h, and complete dissolution was achieved after 3 h (Fig. 4d and **g**). These outcomes align with the enhanced water solubility of IVM in the presence of surfactants. The dermis is a water-rich skin layer, and the water content progressively increases due to the transdermal hydration gradient (Björklund et al. 2010). The faster dissolution in the case of F2 and F3 compared to F1 may contribute to a rapid release of IVM.

The penetration and permeation of IVM through the skin were evaluated in an ex vivo dermatokinetic study. The skin deposition and permeation efficiency of IVM were compared for F1, F2, F3 DMAPs and efacti® cream (Fig. 5). The results of the dermatokinetic investigation were analysed in terms of percentage delivery efficiency (DE%), which is related to the IVM content in each DMAP formulation. Additionally, the effective amount of IVM deposited in the skin or permeated through the skin (µg) was assessed, independent of the IVM content in DMAPs.

The highest IVM delivery DE% at 24 h was observed for F1, reaching approximately 75% (equal to approximately 1745 µg), with predominant accumulation in the epidermis (50%, equal to approximately 1257 µg). There was no transdermal delivery of IVM detected into the receptor compartment. However, F2 resulted in the greatest amount of IVM deposited in the skin (F1 = 1456.35 ± 266.90 µg; F2 = 2165.24 ± 130.13; F3 = 1684.74 ± 212.09 µg), most of which was in the epidermal layer (1966.48 ± 130.13 µg) (Fig. 5d and **e**). F3 exhibited the lowest IVM DE% at approximately 50% (equal to approximately 1600 µg) (Fig. 5f). In the case of F2 and F3, a burst effect was evident from 1 to 3 h, minimal in the case of F1 (Fig. 5i). The more rapid onset of action of F2 and F3 compared to F1 is a result of faster dissolution in the skin (Fig. 5), which is related to the presence of surfactants. Regarding the control group, IVM cream, we observed that this only led to IVM delivery into the epidermis and dermis with a very low DE% at 24 h (5%, equal to approximately 132 µg) compared to the DMAP formulations. Moreover, there was no measurable transdermal delivery of IVM into the receptor compartment as shown in Fig. 5c. This result suggests that the DMAP platform is superior in delivering a higher amount of IVM into the skin strata compared to passive permeation of IVM *via* cream

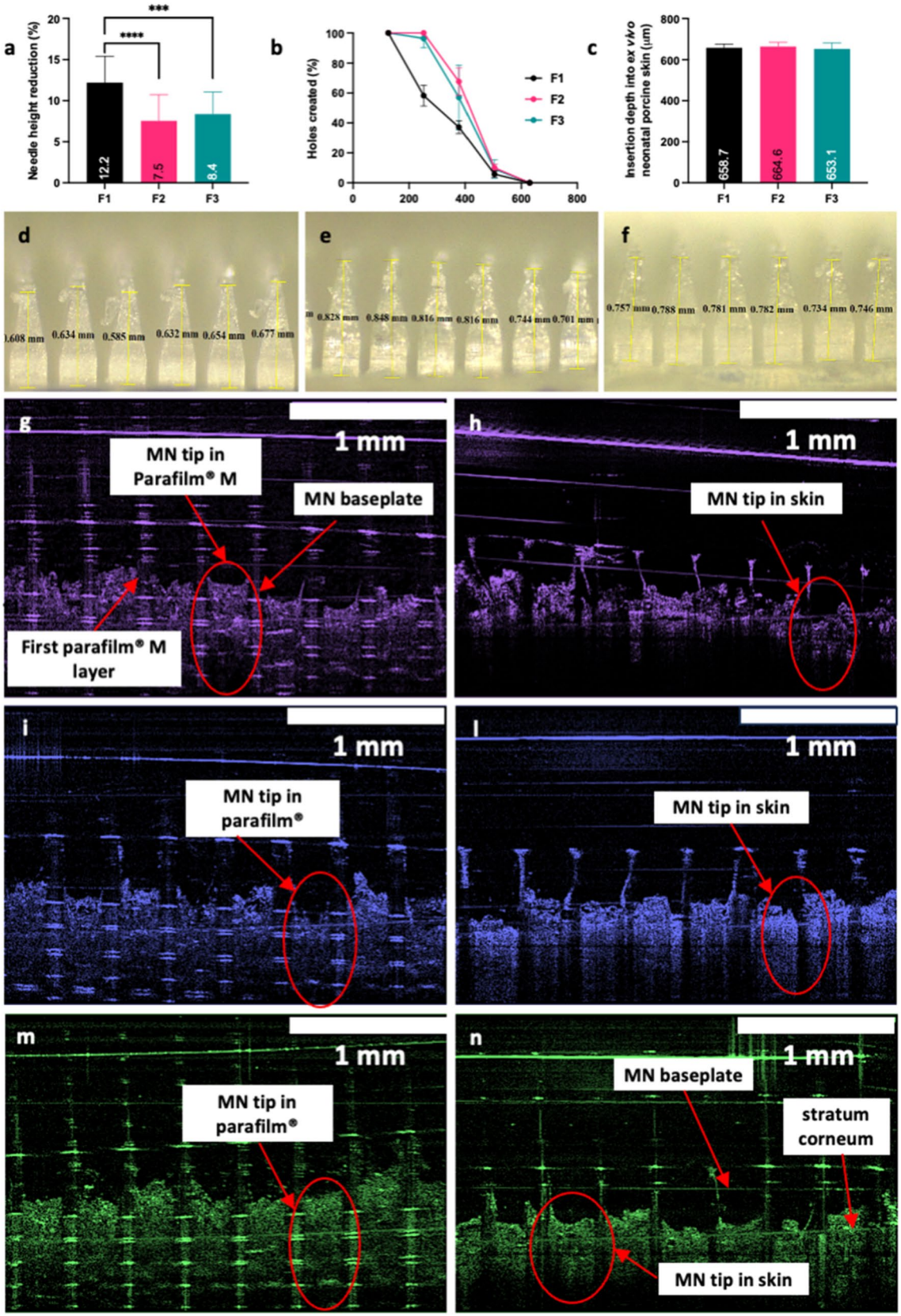

Fig. 3 Mechanical characterisation of DMAPs. **a**: Percentage needle height reduction after compression (32 N, 30 s) against a flat surface (means + SD, $n = 20$). **b**: Insertion capacity of DMAPs in Parafilm® M strata (means ± SD, $n = 3$). **c**: Ex vivo insertion capacity of DMAPs in full-thickness neonatal porcine skin (means + SD, $n = 20$). **g-n**: Optical Coherence Tomography (OCT) analyses of insertion in Parafilm® M **(g, i, m)** and skin **(h, l, n)** for F1 **(g-h)**, F2 **(i, l)** and F3 **(m, n)**

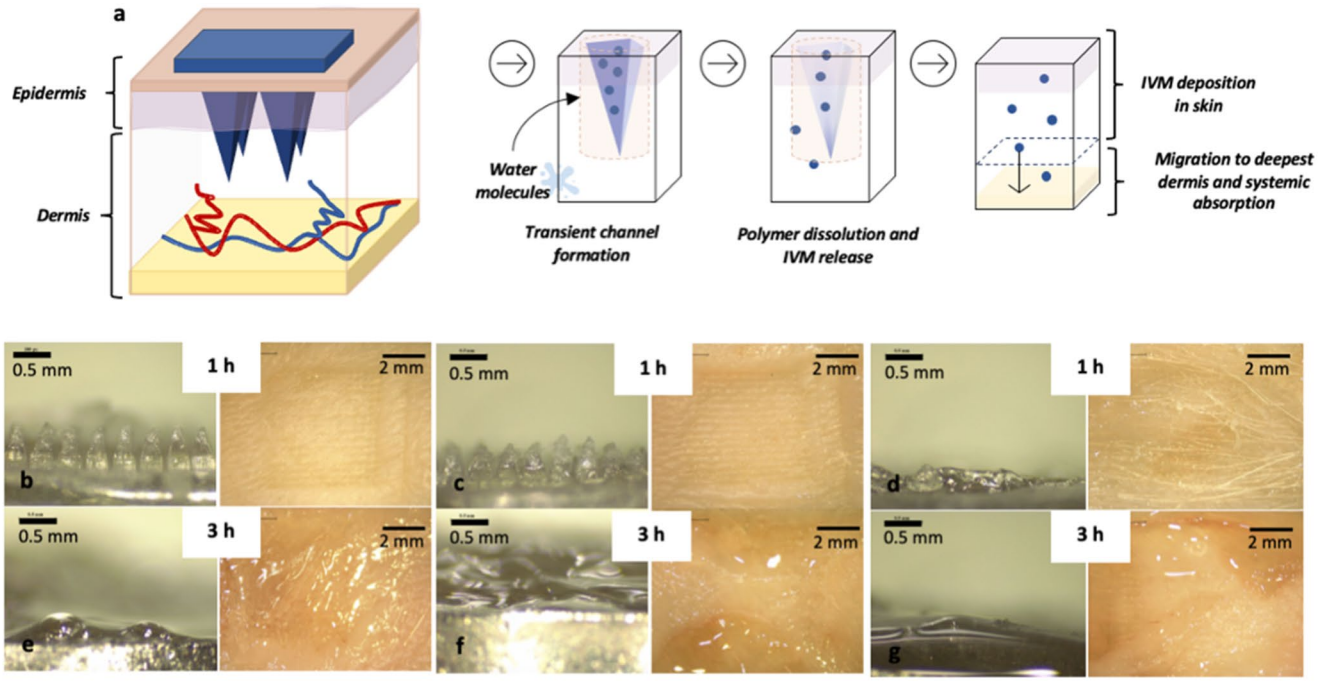

Fig. 4 Dissolution of DMAPs in the skin. a: illustration of the mechanism of dissolution. **b-d**: dissolution of F1, F2 and F3, respectively, after 1 h of ex vivo insertion in full-thickness porcine skin. **e-g**: dissolution of F1, F2 and F3, respectively, after 3 h of ex vivo insertion in full-thickness porcine skin

vehicle, highlighting the potential of DMAPs in improving the delivery of IVM for rosacea treatment.

Surfactants, acting as permeation enhancers, may modify the arrangement of the highly ordered intercellular lipid structure in the upper epidermis, interact with the intercellular domain of proteins, induce conformational modifications, and increase drug partitioning (Kim and Choi 2021; Yang et al. 2022). The enhanced water solubility of IVM due to surfactants further increased its migration through the skin compared to surfactant-free formulations, facilitated by the transdermal hydration gradient (Morin et al. 2020). Additionally, IVM dispersion formulated with surfactants showed a significantly smaller size compared to pure aqueous dispersion ($p < 0.05$), a crucial factor in increasing tissue permeation due to the larger surface area. Larger particles or particle aggregates, on the other hand, tend to deposit in the skin, hindering permeation to deeper tissues (Lim et al. 2019; Kim et al. 2021). However, a limitation of F2 and F3 was observed as these formulations facilitated IVM permeation to the receptor compartment at 24 h, indicating a higher likelihood of systemic circulation delivery in vivo (Fig. 5c). Considering the advantages and drawbacks of the three DMAP formulations, F2 emerges as the most promising candidate for enhancing IVM-based rosacea therapy and was thus selected for further biological studies.

Biological evaluations

The biocompatibility of both IVM-loaded DMAPs and blank DMAP formulations was assessed by evaluating the survival of Human epidermal keratinocytes using the MTT cell viability assay. As depicted in Fig. 6a, the results indicated that both F2 formulations had no adverse effects on cell viability after 72 h (blank DMAPs = 103.7%±1.6; IVM-loaded DMAPs = 97.4%±3.4) compared to the control. This finding was further supported by live and dead staining (Fig. 6h), where no dead cells were observed, and DNA cell content remained unaffected (Fig. 6b) (blank DMAPs = 100.3%±2.45; IVM-loaded DMAPs = 100.3%±2.2). These results indicate that the formulation did not compromise the keratinocytes' viability, plasma membrane integrity, or proliferation. The dose of IVM used in the formulation may explain these findings, as previous literature has reported the beneficial effects of IVM, with a low probability of adversely affecting skin cells (Thibaut de Ménonville et al. 2017; Sansare and Kanavaje 2019; Manca et al. 2021). From a clinical perspective, these data suggest that this fabricated DMAPs is unlikely to cause significant toxicity to the skin.

Stimulation of keratinocytes with LL-37, known to induce proinflammatory responses similar to rosacea disease (Stein Gold et al. 2014; Thibaut de Ménonville et al. 2017), was examined concerning the release of IL1-β, IL-8,

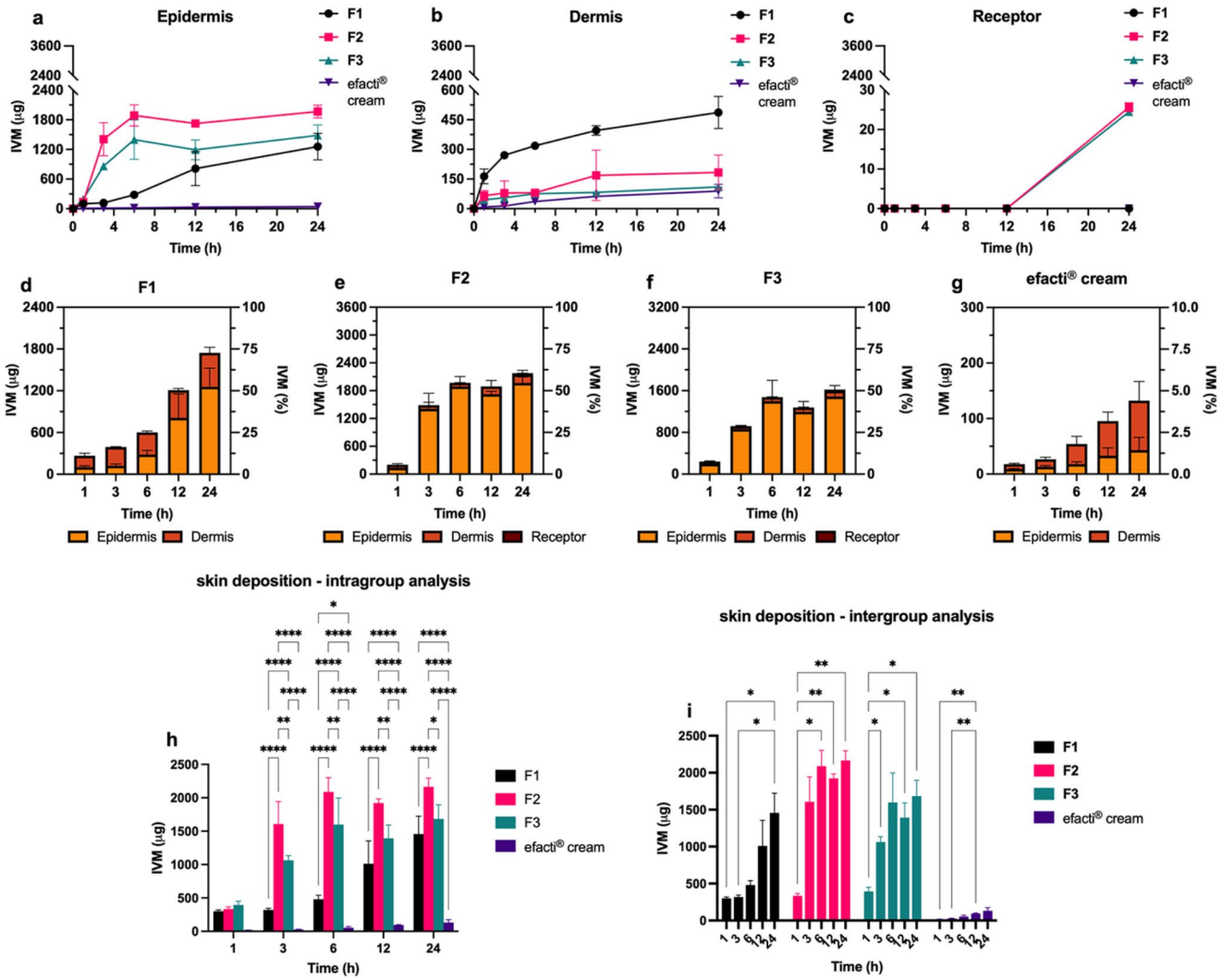

Fig. 5 Ex vivo dermatokinetic study of DMAPs across full-thickness neonatal porcine skin. **a-b**: deposition profile of IVM from F1, F2 and F3 in epidermis and dermis, respectively (means ± SD, $n = 3$). **c**: skin permeation profile of IVM from F1, F2 and F3 (means ± SD, $n = 3$). **d-g**: sum of IVM deposited in the skin (epidermis and dermis) and permeated through the skin from F1, F2 and F3, respectively (means + SD, $n = 3$). The effective amount of IVM (µg) is plotted in the first *y-axis*; IVM percentage delivery efficiency is plotted in the second *y-axis* (means + SD, $n = 3$). **h-i**: statistical analyses of IVM skin deposition (epidermis and dermis) intragroups (**g**) and intergroups (**h**) (means + SD, $n = 3$)

TNF-α, CXCL1, and CXCL2 on IVM-loaded MAPs and blank MAPs. As anticipated, LL-37 significantly increased the release of all cytokines and chemokines studied ($p < 0.05$) (Fig. 6c-h). However, only IVM-loaded DMAPs demonstrated a reversal in the production of proinflammatory cytokines (IL1-β, IL-8, TNF-α) and chemokines (CXCL1 and CXCL2) in keratinocytes following LL-37 treatment. These findings suggest that IVM-loaded DMAPs may potentially counteract the inflammatory effects associated with rosacea. The role of the cathelicidin innate immune pathway, specifically LL-37, in the development of rosacea has been well-established (Gerber et al. 2011; Thibaut de Ménonville et al. 2017; Suhng et al. 2018; Kan et al. 2020). Inhibition of cathelicidin has been proposed as a potential therapeutic approach for rosacea patients, and agents that can inhibit the effects of LL-37 may have a significant impact on reducing inflammation associated with rosacea (Reinholz et al. 2012; Suhng et al. 2018; Lohova et al. 2020; Kan et al. 2020).

The findings from this study suggest that IVM-loaded DMAPs may act by modulating the production of proinflammatory cytokines and chemokines, thereby preventing the activation of inflammatory pathways involved in the pathophysiology of rosacea. Notably, the release of IL1-β, IL-8, TNF-α, CXCL1, and CXCL2 from IVM-loaded F2 treated with LL-37 was lower compared to blank DMAPs, indicating an inhibitory effect (Fig. 6c-h). This suggests that IVM-loaded DMAPs has a more substantial impact on the cathelicidin immune pathway, which is consistent with

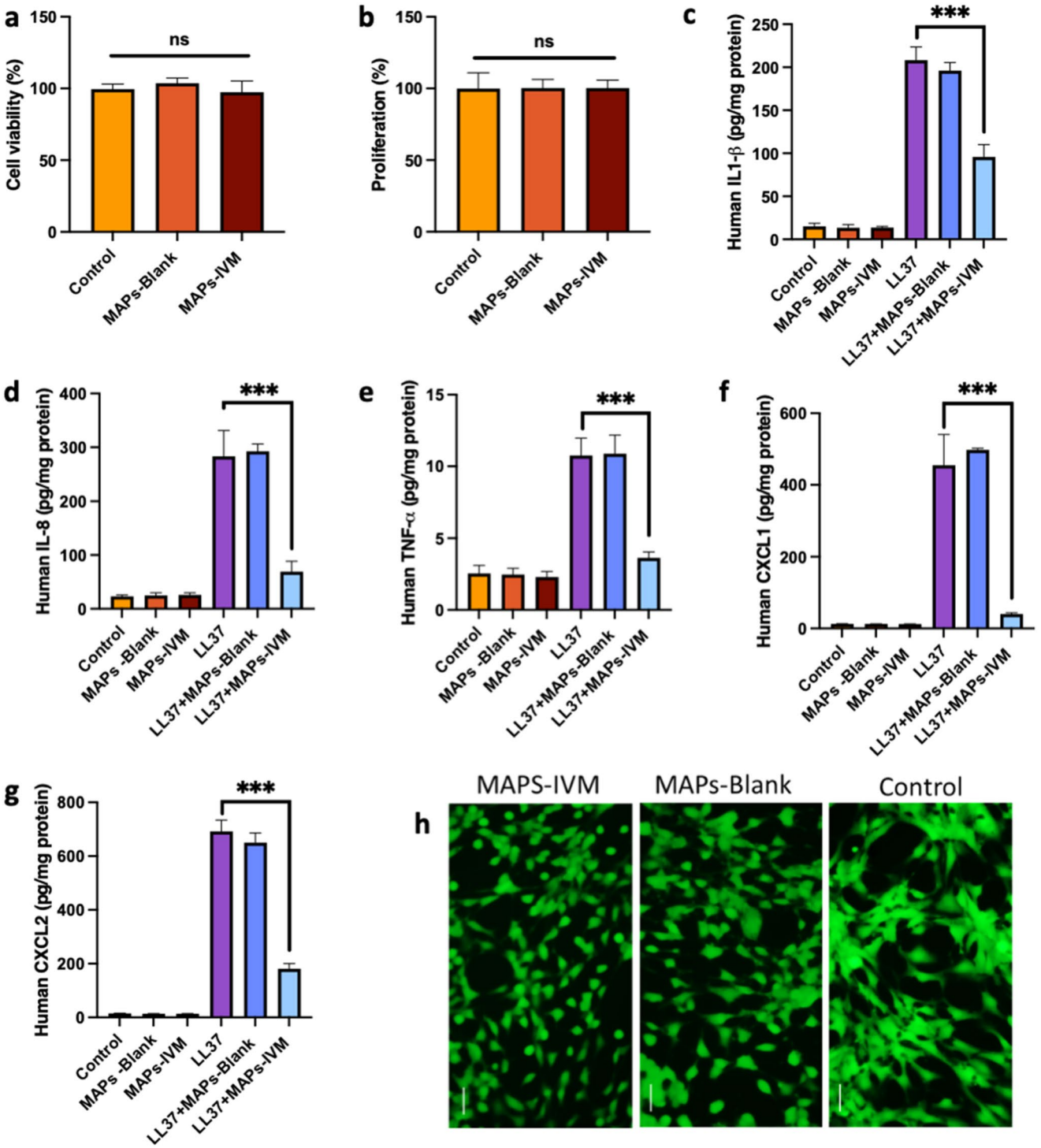

Fig. 6 Keratinocytes cell viability and proliferation on IVM-loaded and blank DMAPs (means + SD, $n = 3$). **a**: MTT assay results show the percentage of viable cells after a culture period of 72 h. **b**: PicoGreen assay results show the total DNA content of cells on control/coverslip, IVM-loaded and blank F2 DMAPs cultured for 72 h (means + SD, $n = 3$). **c-g**: Changes of proinflammatory cytokine and chemokines expression after LL-37 treated human keratinocytes. LL-37 increased the production of Interleukin 1-β (IL1- β), Interleukin-8 (IL-8), tumour necrosis factor (TNF)-α, CXCL1 and CXCL2 determined by enzyme-linked immunosorbent assay in human keratinocytes. MAPS-IVM decreased IL1- β, IL-8 and TNF-α, CXCL1 and CXCL2 release; c: IL1- β, d: IL-8 e: TNF-α, f: CXCL1 and, g: CXCL2 concentration. **h**: Live/dead staining of fibroblastic cells on control (plate cells culture), IVM-loaded and blank F2 DMAPs. (Green = FDA (live); red = PI (dead)); scale bar = 100 µm

the results observed with other topical treatments containing IVM for rosacea (Stein Gold et al. 2014; Thibaut de Ménonville et al. 2017). Similar findings have been reported in other studies, demonstrating reductions in IL-1β, IL-8, TNF-α, CXCL1, and CXCL2 levels and improvement in the proinflammatory state (Mascia et al. 2003; Mássimo et al. 2018; Jiang et al. 2020). Overall, these results suggest that IVM-loaded DMAPs effectively inhibits the downstream signalling pathway of cathelicidin and can prevent the inflammatory effects of rosacea triggered by abnormal LL-37 processing, thereby positively impacting the inflammatory cascade associated with rosacea (e.g., decreased secretion of IL1-β, IL-8, TNF-α, and CXCL2).

Conclusion

The presented investigation focused on developing and characterising IVM-loaded DMAPs as an alternative therapy for rosacea, aiming to provide an efficient alternative to the currently marketed cream. DMAPs were fabricated using a two-layer casting method with a PVA/PVP blend as the backbone polymer. This technique produced sharp DMAPs with excellent penetration capability, reaching up to 650 µm in porcine skin. To address the poor water solubility of IVM, surfactants (Tween® 80 and Soluplus®) were employed, improving the wettability and particle size of the IVM dispersion used for casting DMAPs. The inclusion of surfactants also led to a reduced dissolution time of DMAPs in the skin, resulting in a faster release of IVM into the skin tissue compared to surfactant-free DMAPs. Among the formulations, DMAPs containing Tween® 80 exhibited the highest drug content and IVM deposition in the skin, likely attributed to its higher HLB value, facilitating better interaction with IVM molecules. Furthermore, in vitro studies demonstrated that DMAPs formulated with Tween® 80 did not induce toxicity in skin cells and exhibited positive effects in inhibiting the inflammatory cascade associated with rosacea. These promising outcomes underscore the potential of further research on IVM-loaded DMAPs formulated with Tween® 80 as a viable option for rosacea therapy.

Funding Not applicable.

Data availability The datasets generated during and/or analysed during the current study are available from the corresponding author on reasonable request.

Declarations

Ethical approval and consent to participate Not applicable.

Statement of human and animal rights This article does not contain any studies with human and animal subjects performed by any of the authors.

Conflict of interest All authors (Q. K. Anjani, S. Demartis, N. Moreno-Castellanos, E. Gavini, R. F. Donnelly) declare that they have no conflict of interest.

References

Ahn CS, Huang WW (2018) Rosacea Pathogenesis. Dermatol Clin 36:81–86. https://doi.org/10.1016/j.det.2017.11.001

Anjani QK, Permana AD, Cárcamo-Martínez Á et al (2021) Versatility of hydrogel-forming microneedles in in vitro transdermal delivery of Tuberculosis drugs. Eur J Pharm Biopharm 294–312:294–312. https://doi.org/10.1016/j.ejpb.2020.12.003

Anjani QK, Hidayat A, Sabri B et al (2022a) Soluplus®-based dissolving microarray patches loaded with colchicine: towards a minimally invasive treatment and management of gout. Biomaterials Sci. https://doi.org/10.1039/D2BM01068B

Anjani QK, Sabri AHB, Domínguez-Robles J et al (2022b) Metronidazole nanosuspension loaded dissolving microarray patches: an engineered composite pharmaceutical system for the treatment of skin and soft tissue infection. Biomaterials Adv 140:213073. https://doi.org/10.1016/j.bioadv.2022.213073

Anjani QK, Sabri AHB, McGuckin MB et al (2022c) In Vitro Permeation studies on Carvedilol containing dissolving microarray patches quantified using a Rapid and simple HPLC-UV Analytical Method. AAPS PharmSciTech 23:273. https://doi.org/10.1208/s12249-022-02422-6

Anjani QK, Sabri AHB, Utomo E et al (2022d) Elucidating the impact of surfactants on the performance of dissolving microneedle array patches. Molecular Pharmaceutics acs.molpharmaceut.1c00988-. https://doi.org/10.1021/ACS.MOLPHARMACEUT.1C00988.acs.molpharmaceut.1c00988

Anjani QK, Demartis S, Volpe-Zanutto F et al (2023a) Fluorescence-coupled techniques for Determining Rose Bengal in Dermatological formulations and their application to Ex vivo skin deposition studies. Pharmaceutics 15:408. https://doi.org/10.3390/pharmaceutics15020408

Anjani QK, Pandya AK, Demartis S et al (2023b) Liposome-loaded polymeric microneedles for enhanced skin deposition of rifampicin. Int J Pharm 646:123446–123446. https://doi.org/10.1016/J.IJPHARM.2023.123446

Anjani QK, Sabri AHB, Hamid KA et al (2023c) Tip loaded cyclodextrin-carvedilol complexes microarray patches. Carbohydr Polym 320:121194. https://doi.org/10.1016/j.carbpol.2023.121194

Anjani QK, Volpe-Zanutto F, Hamid KA et al (2023d) Primaquine and chloroquine nano-sized solid dispersion-loaded dissolving microarray patches for the improved treatment of malaria caused by

Plasmodium Vivax. J Controlled Release 361:385–401. https://doi.org/10.1016/j.jconrel.2023.08.009
Anjani QK, Cárcamo-Martínez Á, Wardoyo LAH et al (2024) MAP-box: a novel, low-cost and easy-to-fabricate 3D-printed box for the storage and transportation of dissolving microneedle array patches. Drug Deliv Transl Res 14:208–222. https://doi.org/10.1007/s13346-023-01393-w
Ashour DS (2019) Ivermectin: from theory to clinical application. Int J Antimicrob Agents 54:134–142. https://doi.org/10.1016/j.ijantimicag.2019.05.003
Attia MS, Elshahat A, Hamdy A et al (2023) Soluplus® as a solubilizing excipient for poorly water-soluble drugs: recent advances in formulation strategies and pharmaceutical product features. J Drug Deliv Sci Technol 84:104519. https://doi.org/10.1016/j.jddst.2023.104519
Barnes TM, Mijaljica D, Townley JP et al (2021) Vehicles for Drug Delivery and Cosmetic Moisturizers: Review and Comparison. Pharmaceutics 13:2012. https://doi.org/10.3390/pharmaceutics13122012
Björklund S, Engblom J, Thuresson K, Sparr E (2010) A water gradient can be used to regulate drug transport across skin. J Controlled Release 143:191–200. https://doi.org/10.1016/j.jconrel.2010.01.005
Cárcamo-Martínez Á, Mallon B, Anjani QK et al (2021) Enhancing intradermal delivery of tofacitinib citrate: comparison between powder-loaded hollow microneedle arrays and dissolving microneedle arrays. Int J Pharm 593. https://doi.org/10.1016/j.ijpharm.2020.120152
Chen J, Ren H, Zhou P et al (2022) Microneedle-mediated drug delivery for cutaneous diseases. Front Bioeng Biotechnol 10
Cribier B (2011) Pathophysiology of rosacea: redness, telangiectasia, and rosacea. Ann De Dermatologie et de Vénéréologie 138:S184–S191. https://doi.org/10.1016/S0151-9638(11)70088-6
Deeks ED (2015) Ivermectin: a review in Rosacea. Am J Clin Dermatol 16:447–452. https://doi.org/10.1007/s40257-015-0150-8
Demartis S, Anjani QK, Volpe-Zanutto F et al (2022) Trilayer dissolving polymeric microneedle array loading Rose Bengal transfersomes as a novel adjuvant in early-stage cutaneous melanoma management. Int J Pharm 627. https://doi.org/10.1016/j.ijpharm.2022.122217
Domínguez-Robles J, Cuartas-Gómez E, Dynes S et al (2023) Poly(caprolactone)/lignin-based 3D-printed dressings loaded with a novel combination of bioactive agents for wound-healing applications. Sustainable Mater Technol 35:e00581–e00581. https://doi.org/10.1016/J.SUSMAT.2023.E00581
Gerber PA, Buhren BA, Steinhoff M, Homey B (2011) Rosacea: the Cytokine and Chemokine Network. J Invest Dermatology Symp Proc / Soc Invest Dermatology Inc [and] Eur Soc Dermatological Res 15:40–40. https://doi.org/10.1038/JIDSYMP.2011.9
Gowda BHJ, Ahmed MG, Hani U et al (2023) Microneedles as a momentous platform for psoriasis therapy and diagnosis: a state-of-the-art review. Int J Pharm 632:122591. https://doi.org/10.1016/j.ijpharm.2023.122591
Hmingthansanga V, Singh N, Banerjee S et al (2022) Improved topical drug delivery: role of Permeation enhancers and Advanced approaches. Pharmaceutics 14:2818. https://doi.org/10.3390/pharmaceutics14122818
Jiang Y, Tsoi LC, Billi AC et al (2020) Cytokinocytes: the diverse contribution of keratinocytes to immune responses in skin. JCI Insight 5. https://doi.org/10.1172/JCI.INSIGHT.142067
Jung JH, Jin SG (2021) Microneedle for transdermal drug delivery: current trends and fabrication. J Pharm Investig 51:503–517. https://doi.org/10.1007/s40005-021-00512-4
Kan HL, Wang CC, Cheng YH et al (2020) Cinnamtannin B1 attenuates rosacea-like signs via inhibition of pro-inflammatory cytokine production and down-regulation of the MAPK pathway. PeerJ 8:e10548–e10548. https://doi.org/10.7717/PEERJ.10548/SUPP-3
Karthikeyan K, Aishwarya M, Elayaperumal S (2022) Effectiveness of topical 0.5% Ivermectin Shampoo in the treatment of pediculosis capitis among School-going female children. Int J Trichology 14:55–59. https://doi.org/10.4103/ijt.ijt_157_20
Khan KU, Minhas MU, Badshah SF et al (2022) Overview of nanoparticulate strategies for solubility enhancement of poorly soluble drugs. Life Sci 291:120301. https://doi.org/10.1016/j.lfs.2022.120301
Kim HS (2020) Microbiota in Rosacea. Am J Clin Dermatol 21:25–35. https://doi.org/10.1007/s40257-020-00546-8
Kim EJ, Choi DH (2021) Quality by design approach to the development of transdermal patch systems and regulatory perspective. J Pharm Investig 51:669–690. https://doi.org/10.1007/s40005-021-00536-w
Kim Y-S, Lee K-W, Kim J-S et al (2019) Regional thickness of facial skin and superficial fat: application to the minimally invasive procedures. Clin Anat 32:1008–1018. https://doi.org/10.1002/ca.23331
Kim NA, Oh HK, Lee JC et al (2021) Comparison of solubility enhancement by solid dispersion and micronized butein and its correlation with in vivo study. J Pharm Investig 51:53–60. https://doi.org/10.1007/s40005-020-00486-9
Li W, Li S, Fan X, Prausnitz MR (2021) Microneedle patch designs to increase dose administered to human subjects. J Controlled Release 339:350–360. https://doi.org/10.1016/j.jconrel.2021.09.036
Lim J-H, Na Y-G, Lee H-K et al (2019) Effect of surfactant on the preparation and characterization of gemcitabine-loaded particles. J Pharm Investig 49:271–278. https://doi.org/10.1007/s40005-018-0402-8
Lohova E, Pilmane M, Rone-Kupfere M et al (2020) Characterization of Pro- and Anti-Inflammatory Tissue Factors in Rosacea: A Pilot study. Cosmetics 2020, Vol 7, Page 82 7:82–82. https://doi.org/10.3390/COSMETICS7040082
Ma Y, Li L, Chen J et al (2020) Distinguishing rosacea from sensitive skin by reflectance confocal microscopy. Skin Res Technol 26:671–674. https://doi.org/10.1111/srt.12851
MacLeod DT, Cogen AL, Gallo RL (2009) Skin Microbiology. Encyclopedia of Microbiology. Elsevier, pp 734–747
Manca ML, Manconi M, Meloni MC et al (2021) Nanotechnology for Natural Medicine: Formulation of Neem Oil Loaded Phospholipid vesicles modified with Argan Oil as a strategy to protect the skin from oxidative stress and promote Wound Healing. https://doi.org/10.3390/ANTIOX10050670. Antioxidants 10:
Marmur A, Della Volpe C, Siboni S et al (2017) Contact angles and wettability: towards common and accurate terminology. Surf Innovations 5:3–8. https://doi.org/10.1680/jsuin.17.00002
Martel JL, Miao JH, Badri T (2024) Anatomy, Hair Follicle. In: StatPearls. StatPearls Publishing, Treasure Island (FL)
Martin RJ, Robertson AP, Choudhary S (2021) Ivermectin: An Anthelmintic, an insecticide, and much more. Trends Parasitol 37:48–64. https://doi.org/10.1016/j.pt.2020.10.005
Mascia F, Mariani V, Girolomoni G, Pastore S (2003) Blockade of the EGF receptor induces a deranged chemokine expression in keratinocytes leading to enhanced skin inflammation. Am J Pathol 163:303–312. https://doi.org/10.1016/S0002-9440(10)63654-1
Mássimo I, Velázquez Perdomo L, Ibarra SM et al (2018) CONSENSO ARGENTINO DIAGNÓSTICO DE ROSÁCEA EN LA INFANCIA Argentine consensus diagnosis of rosacea in children. 13:159–176
Mathachan SR, Sardana K, Khurana A (2021) Current use of Ivermectin in Dermatology, Tropical Medicine, and COVID-19: an update on Pharmacology, uses, proven and varied proposed mechanistic action. Indian Dermatology Online J 12:500. https://doi.org/10.4103/idoj.idoj_298_21

Menditto E, Orlando V, De Rosa G et al (2020) Patient Centric Pharmaceutical Drug Product Design—the impact on Medication Adherence. Pharmaceutics 12:44. https://doi.org/10.3390/pharmaceutics12010044

Morin M, Ruzgas T, Svedenhag P et al (2020) Skin hydration dynamics investigated by electrical impedance techniques in vivo and in vitro. Sci Rep 10:17218. https://doi.org/10.1038/s41598-020-73684-y

Ní Raghallaigh S, Bender K, Lacey N et al (2012) The fatty acid profile of the skin surface lipid layer in papulopustular rosacea: fatty acid profile in papulopustular rosacea. Br J Dermatol 166:279–287. https://doi.org/10.1111/j.1365-2133.2011.10662.x

Õmura S, Crump A (2004) The life and times of ivermectin — a success story. Nat Rev Microbiol 2:984–989. https://doi.org/10.1038/nrmicro1048

Paiva-Santos AC, Gonçalves T, Peixoto D et al (2023) Rosacea Topical Treatment and Care: from traditional to New Drug Delivery systems. Mol Pharm 20:3804–3828. https://doi.org/10.1021/acs.molpharmaceut.3c00324

Paredes AJ, Volpe-Zanutto F, Permana AD et al (2021) Novel tip-loaded dissolving and implantable microneedle array patches for sustained release of finasteride. Int J Pharm 606:120885. https://doi.org/10.1016/j.ijpharm.2021.120885

Qu F, Geng R, Liu Y, Zhu J (2022) Advanced nanocarrier- and microneedle-based transdermal drug delivery strategies for skin diseases treatment. Theranostics 12:3372–3406. https://doi.org/10.7150/thno.69999

Raedler LA (2015) Soolantra (Ivermectin) 1% cream: a Novel, antibiotic-free Agent approved for the treatment of patients with Rosacea. Am Health Drug Benefits 8:122–125

Reinholz M, Ruzicka T, Schauber J (2012) Cathelicidin LL-37: an Antimicrobial peptide with a role in inflammatory skin disease. Ann Dermatol 24:126–126. https://doi.org/10.5021/AD.2012.24.2.126

Saepang K, Li SK, Chantasart D (2021) Passive and iontophoretic transport of pramipexole dihydrochloride across human skin microchannels created by microneedles in vitro. Int J Pharm 609:121092. https://doi.org/10.1016/j.ijpharm.2021.121092

Sansare VA, Kanavaje AM, THE POTENTIAL ADVANTAGES OF LIPID NANOPARTICLES IN TREATMENT OF ACNE (2019) J Appl Pharm Sci Res 6–13. https://doi.org/10.31069/japsr.v2i3.2

Sartawi Z, Blackshields C, Faisal W (2022) Dissolving microneedles: applications and growing therapeutic potential. J Controlled Release 348:186–205. https://doi.org/10.1016/j.jconrel.2022.05.045

Schaller M, Gonser L, Belge K et al (2017) Dual anti-inflammatory and anti-parasitic action of topical ivermectin 1% in papulopustular rosacea. J Eur Acad Dermatol Venereol 31:1907–1911. https://doi.org/10.1111/jdv.14437

Stein Gold L, Kircik L, Fowler J et al (2014) Long-term safety of ivermectin 1% cream vs azelaic acid 15% gel in treating inflammatory lesions of rosacea: results of two 40-week controlled, investigator-blinded trials. J Drugs Dermatol 13:1380–1386

Suhng E, Kim BH, Choi YW et al (2018) Increased expression of IL-33 in rosacea skin and UVB-irradiated and LL-37-treated HaCaT cells. Exp Dermatol 27:1023–1029. https://doi.org/10.1111/EXD.13702

Tekko IA, Vora LK, Volpe-Zanutto F et al (2022) Novel bilayer microarray Patch-assisted long-acting Micro-depot Cabotegravir Intradermal Delivery for HIV Pre-exposure Prophylaxis. Adv Funct Mater 32:2106999. https://doi.org/10.1002/ADFM.202106999

Teodorescu M, Bercea M, Morariu S (2019) Biomaterials of PVA and PVP in medical and pharmaceutical applications: perspectives and challenges. Biotechnol Adv 37:109–131. https://doi.org/10.1016/j.biotechadv.2018.11.008

Thibaut de Ménonville S, Rosignoli C, Soares E et al (2017) Topical Treatment of Rosacea with Ivermectin inhibits Gene expression of Cathelicidin Innate Immune Mediators, LL-37 and KLK5, in reconstructed and Ex vivo skin models. Dermatology Therapy 7:213–225. https://doi.org/10.1007/S13555-017-0176-3/FIGURES/4

van Zuuren EJ, Arents BWM, van der Linden MMD et al (2021) Rosacea: New concepts in classification and treatment. Am J Clin Dermatol 22:457–465. https://doi.org/10.1007/s40257-021-00595-7

Vemuri RC, Gundamaraju R, Sekaran SD, Manikam R (2015) Major Pathophysiological Correlations of Rosacea: A Complete Clinical Appraisal. Int J Med Sci 12:387–396. https://doi.org/10.7150/ijms.10608

Vitore JG, Pagar S, Singh N et al (2023) A comprehensive review of nanosuspension loaded microneedles: fabrication methods, applications, and recent developments. J Pharm Investig 53:475–504. https://doi.org/10.1007/s40005-023-00622-1

Vora LK, Sabri AH, Naser Y et al (2023) Long-acting microneedle formulations. Adv Drug Deliv Rev 201:115055. https://doi.org/10.1016/j.addr.2023.115055

Wang M, Hu L, Xu C (2017) Recent advances in the design of polymeric microneedles for transdermal drug delivery and biosensing. Lab Chip 17:1373–1387. https://doi.org/10.1039/C7LC00016B

Wang X, Yuan S, Jiang B (2019) Wetting process and adsorption mechanism of surfactant solutions on coal Dust Surface. J Chem 2019. https://doi.org/10.1155/2019/9085310

Wicha SG, Märtson A-G, Nielsen EI et al (2021) From therapeutic drug monitoring to Model-Informed Precision Dosing for Antibiotics. Clin Pharmacol Ther 109:928–941. https://doi.org/10.1002/cpt.2202

Yang D, Chen M, Sun Y et al (2021) Microneedle-mediated transdermal drug delivery for treating diverse skin diseases. Acta Biomater 121:119–133. https://doi.org/10.1016/j.actbio.2020.12.004

Yang R, Hong Y, Wang Y et al (2022) The embodiment of the strategy of using active chemicals as excipients in compound preparation. J Pharm Investig 52:1–22. https://doi.org/10.1007/s40005-021-00531-1

Zargari O, Aghazadeh N, Moeineddin F (2016) Clinical applications of topical ivermectin in dermatology. Dermatol Online J 22. https://doi.org/10.5070/D3229032496

Zhang L, Guo R, Wang S et al (2021) Fabrication, evaluation and applications of dissolving microneedles. Int J Pharm 604:120749. https://doi.org/10.1016/j.ijpharm.2021.120749

Zhang W, Zhang W, Li C et al (2022) Recent advances of Microneedles and their application in Disease Treatment. Int J Mol Sci 23:2401. https://doi.org/10.3390/ijms23052401